SECOND EUROPEAN CONFERENCE ON EARTHQUAKE ENGINEERING
AND SEISMOLOGY, ISTANBUL AUG. 25-29, 2014

SEISMIC INELASTIC DISPLACEMENTS IN THE PRESENCE OF NON-VISCOUS DAMPING

Gerardo N. Rocha[1] and Y. H. Chai[2]

ABSTRACT

The seismic response of structures is inevitably influenced by the structure's intrinsic damping, which in essence dissipates a portion of the energy imparted to it by the earthquake ground motion. While exact mechanisms contributing to structural damping are admittedly complex, our ability to accurately model the inherent damping is important, as spectral displacements and hence structural damage are dependent on the damping model. Traditionally, structural damping is assumed to be viscous where the dynamic force resisting the motion is taken to be proportional to the instantaneous velocity. But it is well known that the viscous damping assumption results in energy dissipation that increases linearly with frequency. Evidence however suggests that structural damping tends to be non-viscous with energy dissipation being less strongly influenced by the frequency. In this paper, the energy dissipative characteristic of damping is improved by a non-viscous hereditary model. Specifically, the non-viscous damping force is taken to be dependent on the velocity history and written in the form of a convolution integral using an exponentially decaying kernel function. Numerical techniques for solving the equation of motion incorporating non-viscous damping are illustrated. The model is applied to yielding structural systems to investigate the impact of non-viscous damping on peak displacements. Results are presented in the form of response spectra, comparing the non-viscous damping to the classical viscous damping. In particular, ductility demand, which is important for performance assessment, is determined for both exponential and viscous dampings for various levels of lateral strength reduction, as characterized by the force reduction factor. The so-called "equal-displacement" rule in the long-period range and the "equal-energy" rule in the short-period range will also be assessed in the context of non-viscous damping using a set of far-field and near-fault ground motions. Finally, site conditions and their effects on response spectra are examined for both damping models.

INTRODUCTION

The inherent damping in concrete structures has traditionally been modelled as viscous where the resisting force is taken to be proportional to the instantaneous velocity. Lord Rayleigh introduced this simple model in the 19th century to capture the energy dissipation behaviour of real structures and since then the concept has been widely implemented in structural dynamics (Rayleigh, 1877). Experimental data collected over the past several decades has suggested that structural damping may not be accurately represented by the viscous damping concept where energy dissipation increases linearly with frequency (Adhikari, 2005). Experimental evidence further suggested that structural

[1] Ph.D. Student, Department of Civil & Environmental Engineering University of California, Davis, gnrocha@ucdavis.edu
[2] Professor, Department of Civil & Environmental Engineering University of California, Davis, yhchai@ucdavis.edu

damping tends to be non-viscous with energy dissipation being less strongly influenced by the forcing frequency and also that damping depends on other parameters besides the instantaneous generalized velocity (Adhikari and Wagner, 2003, McTravish and Huges, 1993). Any casual model that assures non-negative energy dissipation can be considered as a potential candidate for structural damping (Adhikari and Wagner, 2003). There has been increased interest in the recent years to develop a non-viscous damping model that can represent the dissipative force in a broader, more general manner compared to the simple viscous damping model (Adhikari and Wagner, 2004). In this paper, the non-viscous damping force is assumed to be related to the velocity history via a convolution integral of the following form (Boltzmann, 1876)

$$F_D(t) = \int_{\tau=0}^{\tau=t} c g(t-\tau)\dot{u}(\tau)d\tau \tag{1}$$

where c is the damping coefficient similar to that of viscous damping, $\dot{u}(\tau)$ represents the velocity as a function of the dummy variable τ and $g(t-\tau)$ is a weighting function assumed to take on an exponential form (Biot, 1995)

$$g(t) = \frac{1}{\alpha} e^{\left(-\frac{t}{\alpha}\right)} \tag{2}$$

where α is a positive-valued parameter, commonly called the relaxation time, having units of time

$$\alpha = \eta T_n \tag{3}$$

where η can be regarded as a memory parameter representing the fraction of the fundamental period to be included in the history, and T_n is the fundamental period.

Current seismic codes prescribe design forces that are significantly lower than the force level required for elastic response, implying that inelastic deformation can be expected to occur at the design level earthquake. Since structural damage is related to the level of inelastic deformation, an accurate prediction of the inelastic displacement demand becomes important, particularly the impact of the non-viscous damping on displacements. To that end, a parameter study of inelastic strength and deformation demands is conducted using a set of ground motions from various earthquakes. More specifically, a total of 204 strong ground motions (near-fault & far-field) from 12 earthquakes with peak ground acceleration greater than or equal to 0.15g were used, and these motions were compiled from the Pacific Earthquake Engineering Research Center (PEER) Ground Motion Database and are listed in Table.1. It should be noted that using multiple recordings from single events may result in bias towards the event with the largest number of recordings. To avoid such bias on the results, events that produce more recordings are weighted in proportion to the number of recordings.

The selected ground motions were recorded on a wide range of soil conditions, and can be classified as hard rock (site class A), rock (site class B), very dense soil and soft rock (site class C), stiff soil profile (site class D), and soft soil profile (site class E) according to the National Earthquake Hazards Reduction Program (NEHRP).

EQUATION OF MOTION

The dynamic system subjected to an earthquake ground motion is modelled by a damped SDOF oscillator shown in Fig.1. The equation of motion is given by

$$m\ddot{u}(t) + F_D(t) + F_S(u,z,t) = f(t) \tag{4}$$

where m is the mass of the oscillator, $u(t)$ is the displacement, F_D and F_S are damping and

Table 1. Database of strong motion records used in the study

Event #	Event	Mag	Mechanism	No of recordings grouped by Site Class				
				A	**B**	**C**	**D**	**E**
1	San Fernando, CA (1971)	6.61	Reverse	2	2	4	2	0
2	Imperial Valley-06, CA (1979)	6.53	Strike-Slip	0	0	2	24	2
3	Morgan Hill, CA (1984)	6.19	Strike-Slip	0	0	6	4	0
4	N. Palm Springs, CA (1986)	6.06	Reverse-Oblique	0	0	4	8	0
5	Whittier Narrows-01, CA (1987)	5.99	Reverse-Oblique	0	2	4	12	0
6	Loma Prieta, CA (1989)	6.93	Reverse-Oblique	0	2	14	10	4
7	Erzican, Turkey (1992)	6.69	Strike-Slip	0	0	0	2	0
8	Landers, CA (1992)	7.28	Strike-Slip	0	0	4	2	0
9	Northridge-01, CA (1994)	6.69	Reverse	4	6	20	26	0
9	Northridge-06, CA (1994)	5.28	Reverse	0	0	2	0	0
10	Kobe, Japan (1995)	6.9	Strike-Slip	0	0	2	8	0
11	Chi-Chi, Taiwan (1999)	7.62	Reverse-Oblique	0	0	10	4	0
12	Duzce, Turkey (1999)	7.14	Strike-Slip	0	0	2	4	0
Total number of records:				6	12	74	106	6

restoring forces, respectively, $f(t)$ is the externally applied force and $z(t)$ is the hysteretic displacement. In adapting Eq.(4) to seismic excitation to yielding systems, the equation of motion is written in mass normalized form as

$$\ddot{u}(t) + 2\xi\omega_n \int_{\tau=0}^{\tau=t} \frac{1}{\alpha} e^{\left(\frac{-t-\tau}{\alpha}\right)} \dot{u}(\tau) d\tau + \chi\omega_n^2 u(t) + (1-\chi)\omega_n^2 z(t) = -\ddot{u}_g(t) \tag{5}$$

where ξ is the damping ratio and $\ddot{u}_g(t)$ is the earthquake ground acceleration.

The restoring force F_S, written in mass normalized form, is assumed to be given by the smoothed Bouc-Wen hysteretic model (Sues et al., 1988)

$$F_S(u,z,t) = \chi\omega_n^2 u(t) + (1-\chi)\omega_n^2 z(t) \tag{6}$$

where ω_n is the undamped circular frequency given by

$$\omega_n = \left(\frac{k}{m}\right)^{1/2} \tag{7}$$

where k is the system initial stiffness. The parameter χ in Eq.(6) represents the ratio of post-yield stiffness to initial yield stiffness.

The hysteretic displacement, $z(t)$, is described by the first order nonlinear differential equation

$$\dot{z}(t) = A\dot{u}(t) - \beta|\dot{u}(t)||z(t)|^{n-1} z(t) - \gamma\dot{u}(t)|z(t)|^n \tag{8}$$

which can be written in compact form as

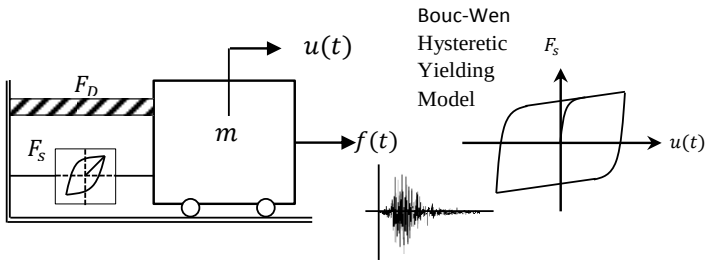

Figure 1. Mechanistic model for non-viscously damped inelastic oscillator

$$\dot{z}(t) = \dot{u}(t)\left\{A - \left|z(t)\right|^n \left(\gamma + \beta \operatorname{sgn}\left(\dot{u}(t)z(t)\right)\right)\right\} \tag{9}$$

where $\operatorname{sgn}(\cdot)$ is the signum function defined as

$$\operatorname{sgn}(x) = \begin{Bmatrix} 1, & x > 0 \\ 0, & x = 0 \\ -1, & x < 0 \end{Bmatrix} \tag{10}$$

The parameters A, β, γ, and n are dimensionless quantities controlling the behavior of the hysteretic model. Values used in this paper follow those in the literature (Ikhouane et al., 2007, Zang et al., 2002, Sues et al., 1988), and are summarized in Table.2. In this paper, we illustrate how the response of the dynamic system described by Eqs. (1), (4), and (8) can be solved via an implicit direct time integration scheme which was proposed by Cortes et al. (2009) but adapted to inelastic systems as characterized by the Bouc-Wen hysteretic model.

DIRECT TIME INTEGRATION FORMULATION FOR INESLATIC SYSTEMS

The direct time integration formulation proposed by Cortes et al. (2009) employs the Laplace transformation of the equation of motion. Eq.(4), along with some maniupulation and followed by inverse Laplace transform, can be converted into a differential equation with time derivative orders higher than two, which can then be solved by a direct time integration scheme. Assuming zero initial conditions, the Laplace transform of the set of equations, namely Eqs. (1), (4), (6), and (8), can be combined into

$$\left(k\chi + \frac{sc}{1+s\alpha} + ms^2\right)U(s) = F(s) + k(\chi - 1)Z(s) \tag{11}$$

where s is the Laplace parameter, $F(s)$ and $Z(s)$ represent the Laplace transform of the resisting force $F_S(t)$ and hysteretic displacement $z(t)$, respectively. Multiplying Eq.(11) by $(1+s\alpha)$ and rearranging

$$\left(\alpha m s^3 + m s^3 + (\alpha k\chi + c)s + k\chi\right)U(s) = (1+s\alpha)F(s) + \left(\alpha k(\chi - 1)s + k(\chi - 1)\right)Z(s) \tag{12}$$

The inverse Laplace transform of Eq.(12) is

$$\alpha m\dddot{u}(t) + m\ddot{u}(t) + (c + \alpha k\chi)\dot{u}(t) + k\chi u(t) = \alpha\dot{f}(t) + f(t) + \alpha k(\chi - 1)\dot{z}(t) + k(\chi - 1)z(t) \tag{13}$$

Table 2. Parameter values for Bouc-Wen hysteretic model used in this study

Parameter	Description	Viscous Damping	Exponential Damping
A	Basic hysteretic shape control	1	1
n	Sharpness of yield	2	2
β	Basic hysteretic shape control	-3 γ	-3 γ
γ	Basic hysteretic shape control	$-0.5\left(F_y/k\right)^{-n}$	$-0.5\left(F_y/k\right)^{-n}$
χ	Ratio of post-yield to initial stiffness	0.012	0.012
η	History dependency of the exponential damping force	---	0.5
α	Relaxation parameter	---	ηT_n
ξ	Damping ratio	0.05	0.05

Eq.(13) is a third-order ODE, which upon the application of backward first and second-order approximations of the derivatives, can be transformed into a second-order ODE. The backward first-order approximations of the first and second derivatives a of a fucntion $p(t)$ are given by

$$\dot{p}(t) = \lim_{h\to 0} \frac{p(t) - p(t-h)}{h} \tag{14}$$

and

$$\ddot{p}(t) = \lim_{h\to 0} \frac{p(t) - 2p(t-h) + p(t-2h)}{h^2} \tag{15}$$

where h is the step size. Thus Eq.(13) may be approximated in discrete form as

$$\begin{aligned} &m\left(1+\frac{\alpha}{h}\right)\ddot{u}_{i+1} + (c+\alpha k\chi)\dot{u}_{i+1} + (k\chi)u_{i+1} \\ &= \left(1+\frac{\alpha}{h}\right)f_{i+1} - \left(\frac{\alpha}{h}\right)f_i + k\left(\chi - \frac{\alpha}{h}(1-\chi) - 1\right)z_{i+1} + \frac{\alpha k}{h}(1-\chi)z_i + \frac{\alpha m}{h}\ddot{u}_i \end{aligned} \tag{16}$$

where z_{i+1} is needed at every time step, which may be determined by solving Eq.(8) using the second-order Runge-Kutta approximation scheme,

$$z_{i+1} = z_i + hK_2 \tag{17}$$

where

$$\left\{\begin{array}{l} K_2 = M\left(t+\frac{1}{2}h, z_i + \frac{1}{2}hK_1\right) \\ K_1 = M(t, z_i) \end{array}\right\} \tag{18}$$

and $M(t, z_i)$ is the evaluation of Eq.(8) at $t = i$, i.e. the current time step. Thus Eq.(16) may be written in equivalent form as a second-order system

$$m_{sys}\ddot{u}_{i+1} + c_{sys}\dot{u}_{i+1} + k_{sys}u_{i+1} = (f_{sys})_{i+1} \tag{19}$$

where

$$\left\{\begin{array}{l} m_{sys} = m\left(1+\frac{\alpha}{h}\right) \\ c_{sys} = (c+\alpha k\chi) \\ k_{sys} = (k\chi) \end{array}\right\} \tag{20}$$

and

$$(f_{sys})_{i+1} = \left(1+\frac{\alpha}{h}\right)f_{i+1} - \left(\frac{\alpha}{h}\right)f_i + k\left(\chi - \frac{\alpha}{h}(1-\chi) - 1\right)z_{i+1} + \frac{\alpha k}{h}(1-\chi)z_i + \frac{\alpha m}{h}\ddot{u}_i \tag{21}$$

Eq.(19) may now be solved by direct integration methods such as the Newmark's constant

acceleration. It has been noted that this formulation may not be valid for systems with more than two exponential damping models and may be affected by low precision (Cortes et al., 2009, Pan and Wang, 2012). In this study, however, the set of equations described by Eqs. (1), (4), (6), and (8), was purposely transformed into a system of first-order differential equations in the following form $\dot{y} = f(t, y)$ so that they can be easily implemented and solved using the ODE solver in Matlab™ (R2012a).

To that end, the damping force, $F_D(t)$, can be transformed into a first-order differential equation by applying the Leibniz rule for differentiation on an integral (Seiber et al., 2008),

$$\dot{F}_D(t) = c\frac{1}{\alpha}\dot{u}(t) - \frac{1}{\alpha}F_D(t) \tag{22}$$

Next, by defining

$$\left\{\begin{array}{rcl} x_1(t) &=& u(t) \\ x_2(t) &=& \dot{u}(t) \\ x_3(t) &=& z(t) \\ x_4(t) &=& \frac{1}{c}F_D(t) \end{array}\right\} \tag{23}$$

the governing equations can be written as a system of first-order differential equations as

$$\left\{\begin{array}{l} \dot{x}_1(t) = x_2(t) \\ \dot{x}_2(t) = -\ddot{u}_g(t) - 2\xi\omega_n x_4(t) - \left(\chi\omega_n^2 x_1(t) + (1-\chi)\omega_n^2 x_3(t)\right) \\ \dot{x}_3(t) = Ax_2(t) - \beta\left|x_2(t)\right|\left|x_3(t)\right|^{n-1}x_3(t) - \gamma x_2(t)\left|x_3(t)\right|^n \\ \dot{x}_4(t) = \frac{1}{\alpha}x_2(t) - \frac{1}{\alpha}x_4(t) \end{array}\right\} \tag{24}$$

which can then be solved via a direct numerical integration method found in most application softwares such as Matlab™.

INELASTIC STRENGTH DEMANDS

The level of inelastic deformation experienced by a system under seismic forces is examined in terms of a displacement ductility factor, μ, which is defined as the ratio of the maximum relative displacement to the yield displacement

$$\mu = \frac{\left|u(t)\right|_{\max}}{u_y} \tag{25}$$

and by a strength reduction factor, R_μ, which is defined as the ratio of the elastic strength demand to the inelastic strength demand,

$$R_\mu = \frac{F_y(\mu = 1)}{F_y(\mu = \mu_T)} \tag{26}$$

where $F_y(\mu = 1)$ is the lateral force required to prevent yielding of the system under a given ground motion and $F_y(\mu = \mu_T)$ is the lateral yield strength required to maintain the displacement ductility

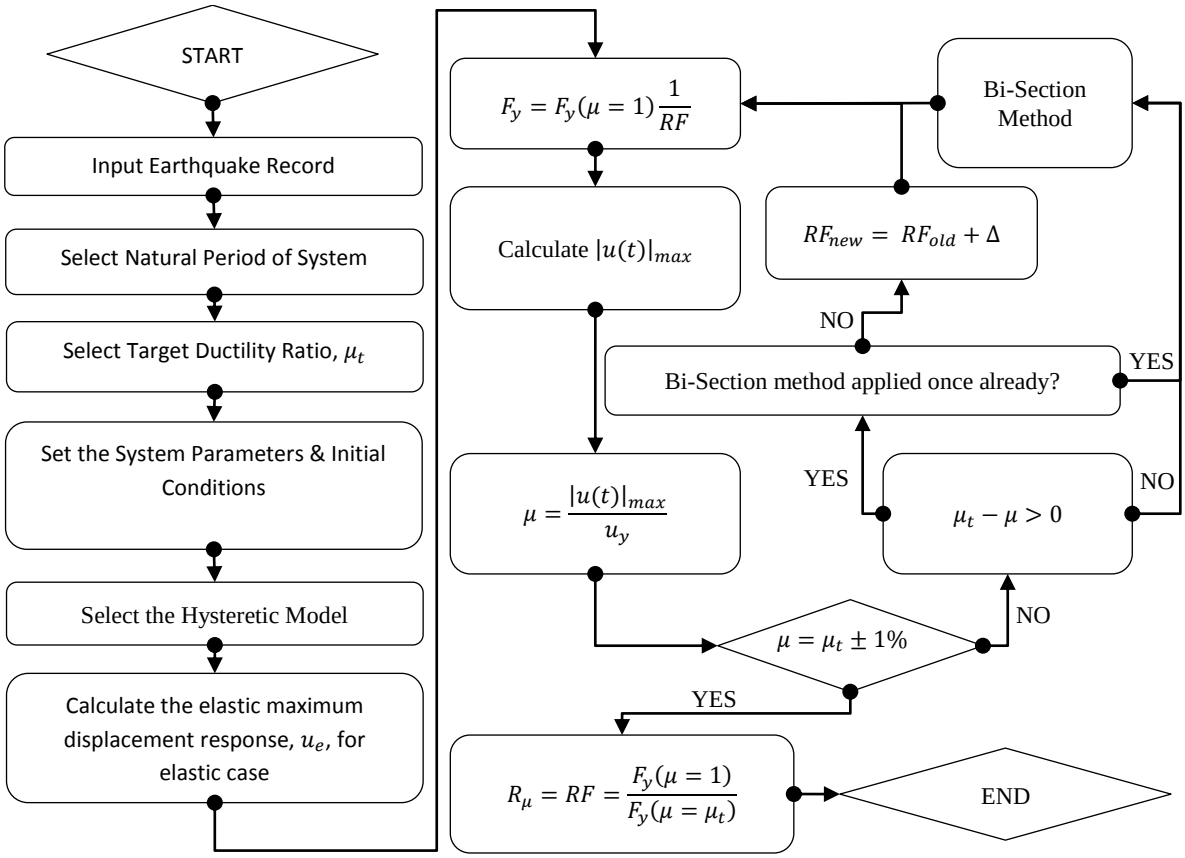

Figure 2. Flow chart for iteration of strength reduction factors for a given target ductility

ratio demand, μ (Miranda and Bertero, 1994).

Inelastic response associated with a target ductility is obtained via an iterative procedure shown by the flowchart in Fig.2. For each earthquake ground motion, the lateral yield strength is varied until the error associated with the computed ductility demand is within 1% of the target ductility. A total of 215 periods, ranging from 0.01 to 5 seconds, were used for each ground motion, and the target ductility ratios were 1, 2, 3, 4, 5, and 6. Results are examined relative to the site conditions for each ground motion.

RESULTS: INELASTIC STRENGTH & DISPLACEMENT DEMANDS

Mean strength spectra of 204 ground motions are plotted in Fig.3 for viscous and exponential damping next to each other for comparison. These spectra are plotted for different soil types and for discrete displacement ductility ratios of $1 \le \mu \le 6$. Fig.3(a-e) corresponds to the mean strength spectra for viscous damping while Fig.3(f-g) corresponds to the mean strength spectra for exponential damping. A value of $\eta = 0.5$ is used for the exponential damping model. It can be seen that the amplitudes and, to a lesser extent, the spectral shapes for elastic response i.e. $\mu = 1$ are quite different for viscous and exponential damping. Their difference is less pronounced for inelastic response, particularly for large ductility demands. It should be noted that the mean strength spectral for soft soils (soil type E) were computed as a function of the period as opposed to period ratios T/Tg, where Tg denotes the ground motion predominant period.

Using the same set of results, mean normalized strength spectra are further plotted in Fig.4 for all five soil types for elastic response $\mu = 1$ and inelastic response $\mu = 4$. It can be seen from Fig.4 that site conditions significantly affect the elastic and inelastic strength spectra and their effects are greater for elastic systems than for inelastic systems. Results obtained in this study for viscous damping are also compared with that published in the literature and are shown in Fig.5 for soil types C and D. Their comparisons indicate good agreement.

Dispersion of strength demands and inelastic displacement demands is also investigated with results for soil type D plotted in Fig.6. The dispersion is measured with the coefficient of variation (COV), which is defined as the ratio of the standard deviation to the mean. It can be seen that the

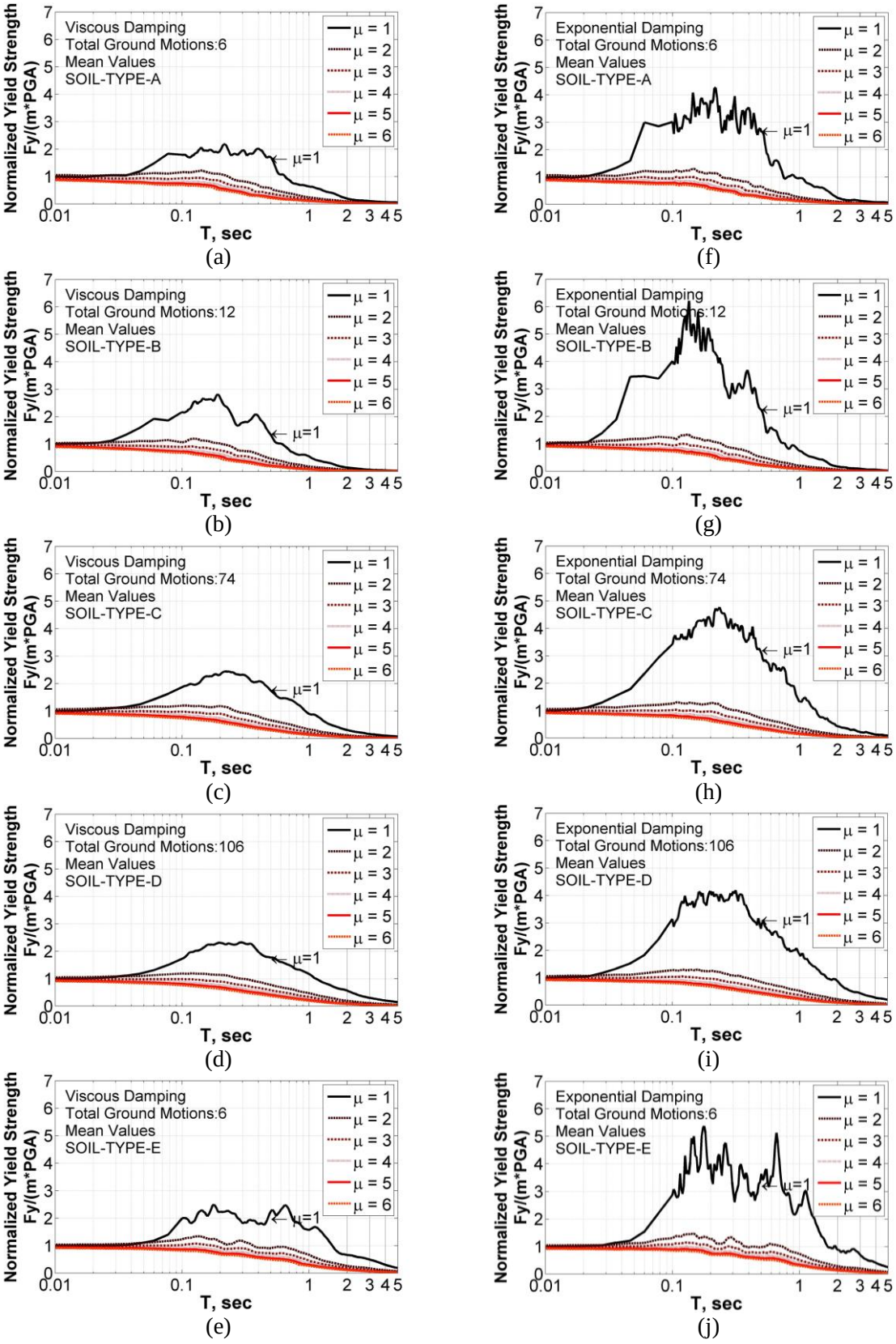

Figure 3. Mean normalized strength demand spectra plots (a-e) correspond to viscous damping while plots (f-j) to exponential damping

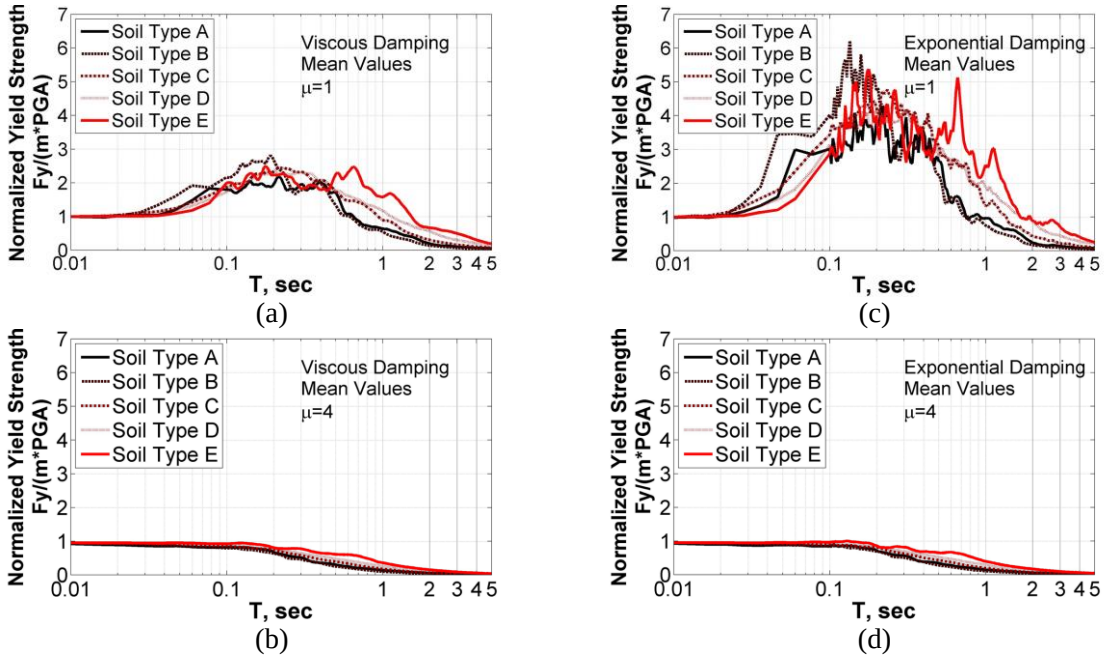

Figure 4. Effects of site conditions on elastic response spectra and on inelastic response spectra for viscous and exponential damping models

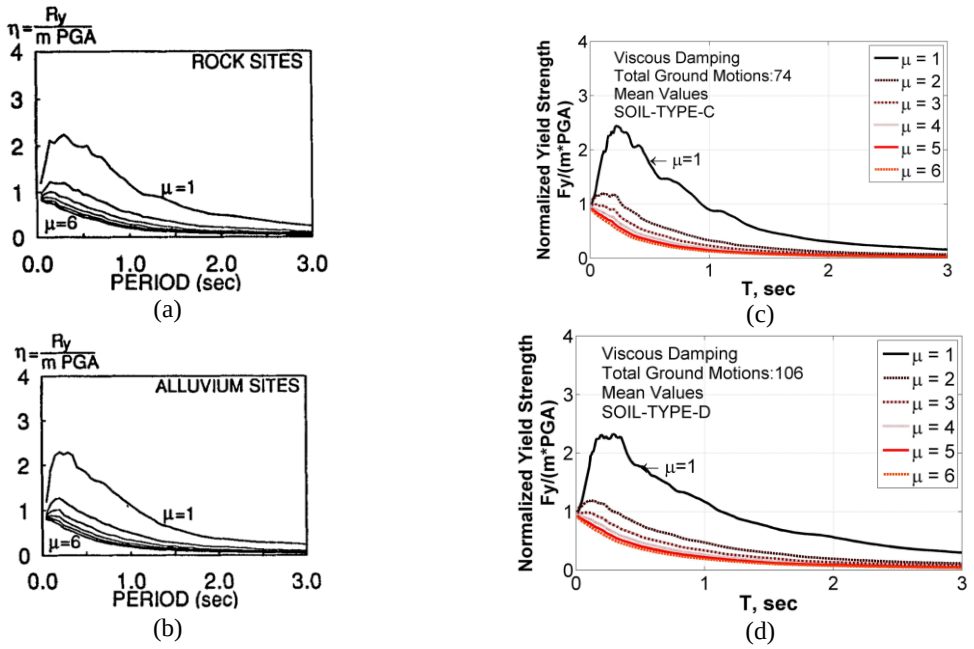

Figure 5. Mean normalized strength demand spectra plots (a-b) were taken from a study done by Miranda (1993) and plots (c-d) correspond to this study

COV for normalized strength demands, Fig.6(a) & Fig.6(c) increases slightly for increasing levels of ductility in the period range between 0.1s to 3.0s. The dispersion of inelastic strength demands do not increase with increasing ductility demands for periods less than 0.1s or greater than 3.0s. This is true for both exponential damping and viscous damping. Fig.6(c) & Fig.6(d) show that the COV for inelastic displacement ratios increases as the level of inelastic deformation increases across the period range from 0.01s to 5.0s.

Mean inelastic displacement ratios for soil type C are plotted in Fig.7. The inelastic displacement ratio is defined as the maximum lateral inelastic displacement demand, $\Delta_{inelastic}$, divided

by the maximum lateral elastic displacement demand, $\Delta_{elastic}$. It can be seen that inelastic displacement demand ratios for viscous and exponential damping are larger than one in the short period region and approximately equal to one for periods longer than 1.0s in the case of viscous damping and longer than 0.3s for exponential damping. In general, in the short period spectral region the maximum inelastic displacements become much larger than maximum elastic displacements as ductility demand increases and as the period decreases. Moreover, it can be seen that inelastic displacement ratios tend towards μ as the period of vibration tends to zero. It is important to note that the level of ductility affects the region where the equal displacement rule is applicable and where it is unconservative. In other words, the limiting period is dependent on the level of ductility. For example, for a ductility ratio of 3, the equal displacement rule is applicable for periods longer than

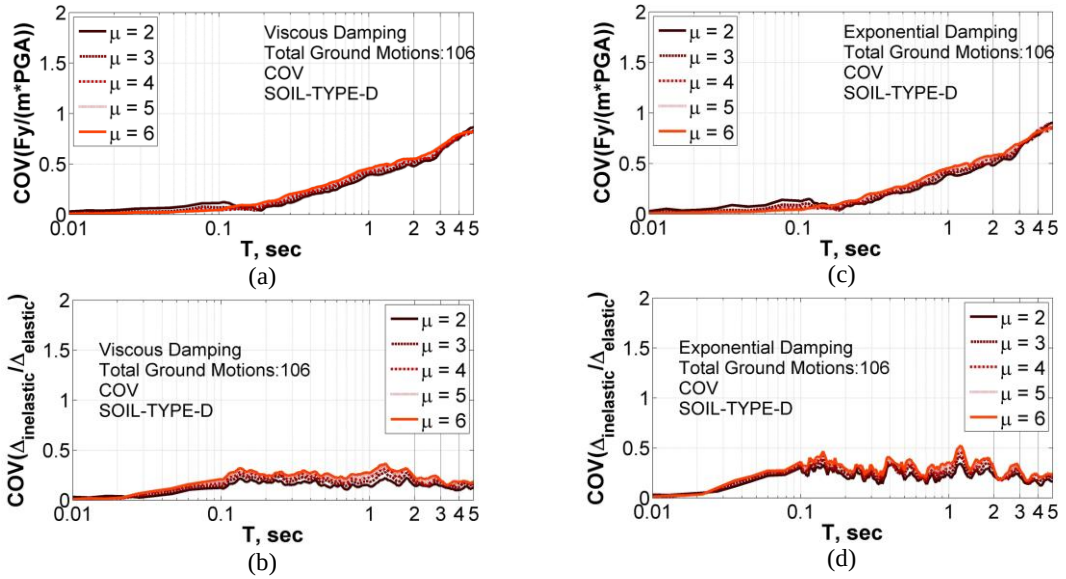

Figure 6. Coefficient of variation of normalized strength demands & inelastic displacement ratios for soil type D

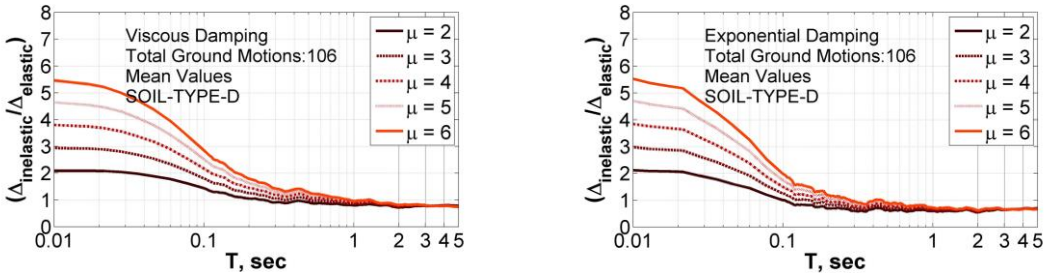

Figure 7. Mean inelastic displacement ratios for soil type D

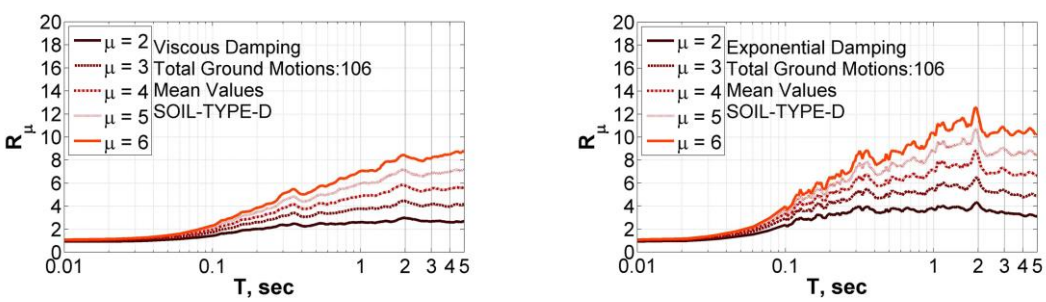

Figure 8. Mean response reduction factors for soil type D

about 0.5s while for a ductility ratio of 5 the equal displacement rule is applicable for periods longer than about 0.9s. Similar observations were made for mean inelastic displacement ratios for site class A, B, C, and E.

Near fault ground motion records were also included in this study. Past studies have shown that strong velocity pulses in the ground motion often occur in near-fault ground motions and the strongest pulses tend to occur closer to the fault normal direction than fault parallel with directivity effects (Somerville et al., 1997). Mean normalized strength spectra are plotted in Fig.9.

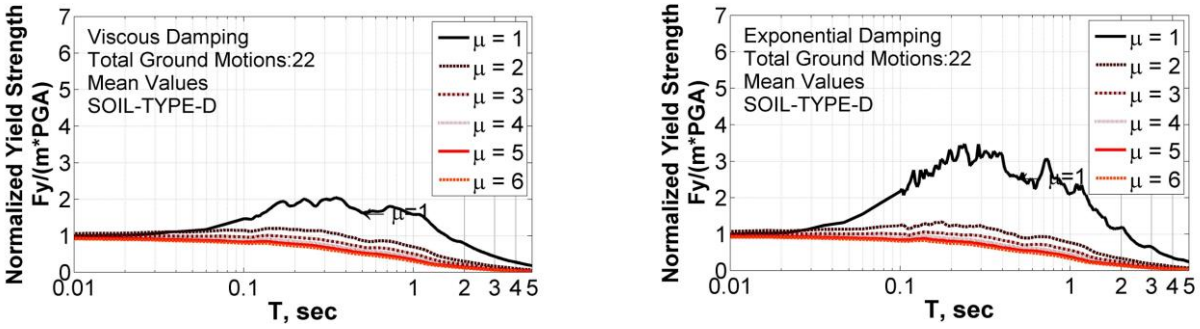

Figure 9. Mean normalized strength demand spectra for near-fault ground motion records for soil type D

CONCLUSIONS

This study investigates the effects of exponential damping on the inelastic strength and inelastic deformation response spectra. Results from a statistical study of both strength and deformation demands of single-degree-of-freedom inelastic systems characterized by the Bouc-Wen hysteretic model when subjected to 204 strong ground motions recorded on different soil conditions are presented. Numerical techniques for solving the equation of motion incorporating exponential damping are also illustrated.

The following conclusions can be made from numerical results of exponential damping:

1. Mean strength spectra amplitudes and, to a lesser extent, the spectral shapes for elastic response i.e. $\mu = 1$ are quite different. Their difference is less pronounced for inelastic response, particularly for large ductility demands.
2. Mean inelastic displacement ratios are characterized by values larger than unity and are both period and ductility dependent in the short period spectral region and period independent for periods larger than 1.0s. Maximum inelastic displacements are on average equal to maximum elastic displacements in the long period spectral region. The period spectral region where the equal displacement rule is applicable is depended on the level of inelastic deformations where the limiting period increases with increasing ductility factors.
3. Site conditions affect the elastic and inelastic strength spectra and their effects are greater for elastic systems than for inelastic systems.
4. Dispersion of mean normalized strength spectra increases as the level of inelastic deformation increases between 0.1-3.0s period range. The dispersion for inelastic displacement ratios increases as the level of inelastic deformation increases.
5. Results presented in this study indicate that exponential damping can be expected to give rise increased inelastic displacements for normal and near-fault ground motions.

REFERENCES

Adhikari S (2008) "Dynamic response characteristics of a nonviscously damped oscillator," *Journal of Applied Mechanics*, 75

Adhikari S (2005) "Qualitative dynamic characteristics of non-viscously damped oscillator," *Proceedings of the Royal Society A*, 461:2269-2288

Adhikari S (2000) Damping models for structural vibrations, Ph.D. Thesis, Cambridge University.

Adhikari S and Wagner N (2004) “Direct time-domain integration method for exponentially damped linear systems,” *Computers and Structures*, 82:2453-2461

Adhikari S and Wagner N (2003) “Symmetric state-space method for a class of nonviscously damped systems,” *AIAA Journal*, 41(5):951-956

Barruetabea J G, Cortes F, Abete J M (2012) “Dynamics of an exponentially damped solid rod: Analytic solution and finite element formulations,” *International Journal of Solids and Structures*, 49(34):590-598

Barruetabea J G, Cortes F, Abete J M (2011) “Influence of nonviscous modes on transient response of lumped parameter systems with exponential damping,” *Journal of Vibration and Acoustics*, 133

Biot M A (1995) “Variational principles in irreversible thermodynamics with application to viscoelasticity,” Phys Rev 97:1463-9

Boltzmann L Z (1876) Theorie der elasticshen Nachwirkung, Progg Ann Phys Chem 7:624:54

Charalampikis A E and Koumousis V K (2009) “A bouc-wen model compatible with plasticity postulates,” *Journal of Sound and Vibration*, 322:954-968

Charalampikis A E and Koumousis V K (2007) “On the response and dissipated energy of bouc-wen hystretic model,” *Journal of Sound and Vibration*, 309:887-895

Cortes F, Mateos M, Elejabarrieta M J (2009) “A direct integration formulation for exponentially damped structural systems,” *Computers Structures*, 87(56):391-394

Han S W, Oh Y H, Lee L H, Foutch D A (1999) Effect of Hysteretic Models on the Inelastic Response Spectra, Civil Engineering Studies, Structural Research Series Report No. 628, Department of Civil and Environmental Engineering, University of Illinois at Urbana-Champaign, October

Ikhouane F, Manosa V, Rodellar J (2007) “Dynamic properties of the hysteretic Bouc-Wen model,” *Systems and Control Letters*, 53(3), 197-205

Ma F, Zhang H, Bockstedte A, Foliente G C, Paevere P (2004) “Parameter analysis of the differential model of hysteresis,” *Transactions of the ASME*, 71, 342–349

MATLAB version R2012a, Natick, Massachusetts: The MathWorks, Inc.

McTavish D J and Hughes P C (1993) “Modeling of Linear Viscoelastic Space Structures” *ASME Journal of Vibration and Acoustics*, 115:103-113.

Miranda E (1993) "Evaluation of Site-Dependent Inelastic Seismic Design Spectra," *Journal of Structural Engineering*, Vol. 119, pp.1319-1338

Miranda E and Bertero V V (1994) "Evaluation of Strength Reduction Factors for Earthquake-Resistant Design," *Earthquake Spectra*, Vol. 10, No, 2.

Pan Y and Wang Y (2012) “Frequency-domain analysis of exponentially damped linear systems,” *Journal of Sound and Vibration*, 322(7):1754-1765 Article in Press

PEER http://peer.berkeley.edu/peer_ground_motion_database/. Pacific Earthquake Engineering Research Center (PEER) Strong Motion Database.

Priestley M J N and Grant D N (2005) "Viscous Damping in Seismic Design and Analysis," *Journal of Earthquake Engineering*, Vol. 9, No, 2

Rayleigh L (1877) Theory of Sound, (two volumes). 2nd ed. New York: Dover Publications. 1945 (re-issue)

Riddell R, Garcia J E, Garces E (2002) "Inelastic deformation response of SDOF system subjected to earthquakes," *Earthquake Engineering and Structural Dynamics*, 31:515-538

Riddell R (1995) "Inelastic Design Spectra Accounting for Soil Conditions," *Earthquake Engineering and Structural Dynamics*, Vol. 24, pp.1491-1510

Riddell R, Hidalgo P, Cruz E (1989), "Response Modification Factors for Earthquake Resistant Design of Short Period Buildings," *Earthquake Spectra*, Vol. 5, No, 3

Riddel R and Newmark N M (1979) Statistical Analysis of the Response of Nonlinear Systems Subjected to Earthquakes, Civil Engineering Studies, Structural Research Series Report No. 468, Department of Civil and Environmental Engineering, University of Illinois at Urbana-Champaign, August

Seiber J, Wagg D J, Adhikari S (2008) “On the interaction of exponential non-viscous damping with symmetric nonlinearities,” *Journal of Sound and Vibration*, 314:1-11

Sengupta P, Li B (2013) “Modified Bouc-Wen model for hysteresis behavior of RC beam-column joints with limited transverse reinforcement,” Engineering Structures, 46:392-406.

Somerville P G (2003) “Magnitude scaling of the near fault rupture directivity pulse,” *Physics of the Earth and Planetary Interiors*, v. 137, no. 1, p. 12.

Sues R H, Mau S T, Wen Y K (1988) “Systems identification of degrading hysteretic restoring forces,” *Journal of Engineering Mechanics*, 144(5):833-846

Yogesh J (2012) Computer Methods for Engineering with MATLAB Applications, CRC Press, Boca Raton, FL, PRINT

Zhang H C, Foliente G C, Yang Y M, Ma F (2002) “Parameter identification of inelastic structures under dynamic loads,” *Earthquake Engineering and Structural Dynamics*, 31:1113-1130